

# Optomechanical tolerancing with Monte Carlo techniques

Victor Genberg\*, Gregory Michels, Gary Bisson  
Sigmadyne, 803 West Ave, Rochester, NY 14611

\*genberg@sigmadyne.com (585) 235-7460

## ABSTRACT

Mechanical tolerances within an optical system can consist of a wide array of variables including machining tolerances, variability in material properties, uncertainty in applied loads, and discrete resolution of actuation hardware. This paper discusses methods to use integrated modeling and Monte Carlo techniques to determine the effect of such tolerances on optical performance so that the allocation of such tolerances is based upon optical performance metrics. With many random variables involved, statistical approaches provide a useful means to study performance metrics. Examples include the effect of mount flatness on surface RMS and Zernike coefficients and the effect of actuator resolution on the performance of an adaptively corrected deformable mirror. Coefficient of thermal expansion and thermal control tolerances impacting both line-of-sight errors and surface RMS errors are also addressed.

**Keywords:** optomechanical tolerances, integrated modeling, Monte Carlo, line-of-sight.

## 1.0 PURPOSE

This paper addresses the following issues in determining meaningful mechanical tolerances in optical systems.

- 1) Use integrated optomechanical analysis to relate mechanical effects to optical performance metrics
- 2) Use Monte Carlo techniques to determine the effect of many random variables on performance statistics

The examples in this paper will use optical performance metrics of line-of-sight errors, surface RMS, and polynomial coefficients.

## 2.0 ANALYSIS

The analyses described in this section are embedded in the SigFit<sup>1</sup> optomechanical analysis software. A general discussion of SigFit is included in section 7.0

### 2.1 Polynomial coefficients

Polynomial coefficients are typically fit to displacement data in a post-processing step<sup>2</sup>. The method is a least squares fit to find the polynomial coefficients which minimize the error defined as,

$$E = \sum_{i=1}^N w_i \left( ds'_i - \sum_{j=1}^M C_j p_{ji} \right)^2,$$

where,

$N$  = the number of nodes,

$w_i$  = weighting coefficient of node  $i$ ,

$M$  = the number of polynomial terms,

$ds'_i$  = surface deformation or optical path difference at node  $i$ ,

$C_j$  = polynomial coefficient for polynomial term  $j$ ,

$p_{ji}$  = value of normalized polynomial function for term  $j$  at node  $i$ .

Taking partial derivatives of  $E$  with respect to each polynomial coefficient and setting each equal to zero leads to a linear system of  $M$  equations for  $M$  unknowns,

$$[H]\{C\} = \{F\},$$

$$H_{jk} = \sum_i w_i p_{ji} p_{ki},$$

$$F_k = \sum_i w_i ds'_i p_{ki},$$

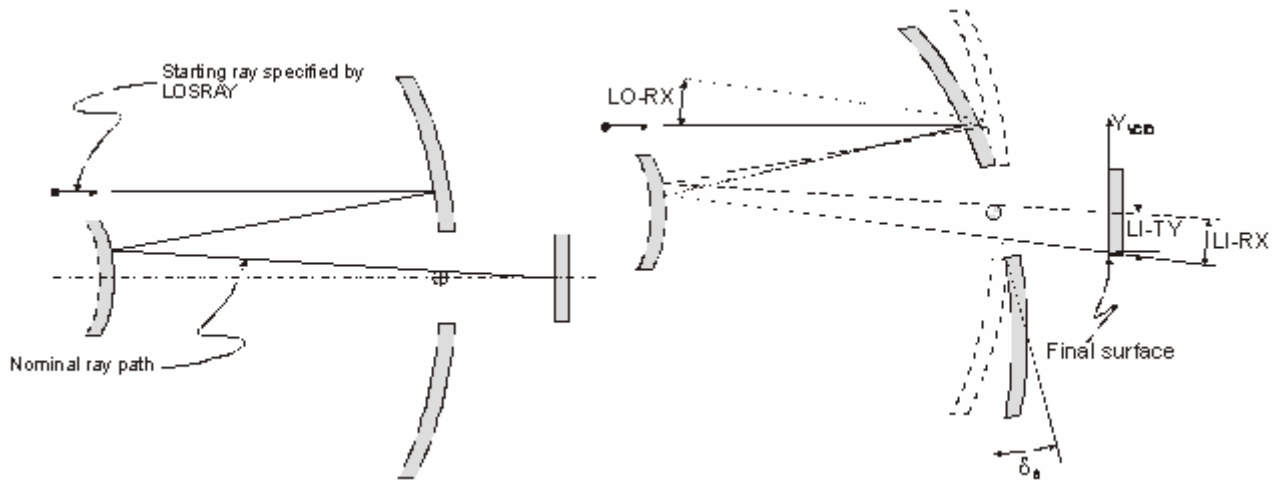
which allows for computation of the coefficients which minimize the error  $E$ . This process can be inverted to write the coefficients as a function of the nodal displacements ( $U = ds'$ ). In SigFit the nodal displacements are modified to include radial correction.

$$\{C\} = [H]^{-1}\{F\} = [A]\{U\}$$

This form is incorporated with the Monte Carlo analysis below. Any of the polynomial types supported by SigFit (shown in section 6) may be used. These polynomials, as well as the rigid-body terms, are all corrected for radial growth, so they can be used to accurately model thermoelastic effects.

## 2.2 Line-of-sight errors

Line-of-sight (LoS) errors are calculated in SigFit from a ray trace algorithm. SigFit calculates the LoS coefficients and automatically performs a rigid-body error check to verify their accuracy. LoS results are presented for both the image space and the object space. Since the rigid-body motion includes radial correction in SigFit, the LoS capability may be used for thermoelastic load cases. Note that an interpolation element like the RBE3 does not correctly account for radial growth of curved optical surfaces.



## 2.3 Monte Carlo analysis

The responses quantities (displacements, polynomial coefficients, surface RMS error, line-of-sight error, etc.),  $U_{ij}$ , are determined by the following equations,

$$V_{ik}^* = V_{Nom_k} + \sigma_k \times \gamma_{ik} \qquad U_{ij} = U_{Nom_j} + \sum_k \frac{dU_j}{dV_k} (V_{ik}^* - V_{Nom_k})$$

where,  $i$  is an index on the Monte Carlo analyses,  $k$  is an index on the variables,  $j$  is an index on the response quantities,  $V_{Nom_k}$  is the nominal or mean value for the  $k^{th}$  variable,  $\sigma_k$  is the uncertainty of the  $k^{th}$  variable, and  $\gamma_{ik}$  is a random number with a mean of 0.0 and an uncertainty of 1.0 with distribution is specified as normal or as uniform for the  $i^{th}$  Monte Carlo analysis and the  $k^{th}$  variable, and  $U_{Nom_j}$  is the nominal or mean value for the  $j^{th}$  response quantity. The partial derivative of the  $j^{th}$  response with respect to the  $k^{th}$  variable is determined from the  $j^{th}$  response of the state used to define the  $k^{th}$  variable minus the  $j^{th}$  response of the specified nominal state. That is,

$$\frac{dU_j}{dV_k} = \frac{U_{jk} - U_{Nom_j}}{V_k - V_{Nom_k}},$$

where,  $U_{jk}$  is the  $j^{th}$  response of the disturbance defining the  $k^{th}$  variable,  $V_k$  is the variable value associated with  $U_{jk}$ .

In SigFit, the response quantities subject to Monte Carlo analysis include:

- 1) rigid-body motion (average surface motion)
- 2) surface RMS error after rigid-body motion subtracted
- 3) polynomial coefficients (using section 2.1)
- 4) line-of-sight errors (using section 2.2)
- 5) adaptively corrected surfaces

The individual variables are subcase response data. Thus any quantity or combination of quantities represented in a finite element model that when varied cause a new response can be a Monte Carlo variable. Any form of input data allowed by SigFit may represent a subcase variable, including regular grid arrays (interferogram arrays from test data), combinations of any type of polynomial in Section 4, and general free format vector data. These variables may be mixed and matched as desired. In fact, a finite element model is not required since SigFit can internally create a mesh for any common optical surface type.

### 3.0 EXAMPLE: MIRROR MOUNT FLATNESS REQUIREMENT

The lightweight mirror in Figure 1 is attached to the metering structure by bipod flexures and a mount plate. The mount plate is bolted to the metering structure, so any non-flatness or non-coplanarity of the attachment plates will cause bending of the mirror. As part of the design specification of the mirror mount plate and metering structure, flatness and coplanarity must be specified. Optomechanical analysis is used to relate mount flatness to the optical requirement on mirror surface RMS. In a finite element model, individual load cases of unit flatness mismatch and non-coplanarity at each mount are applied. In this example, the mismatch at a single mount is represented as three load cases: radial rotation of 0.0001 radian (flatness) (in Figure 2a), circumferential rotation of 0.0001 radian (flatness), and axial displacement of 0.0020 inch (non-coplanarity) (in Figure 2b).

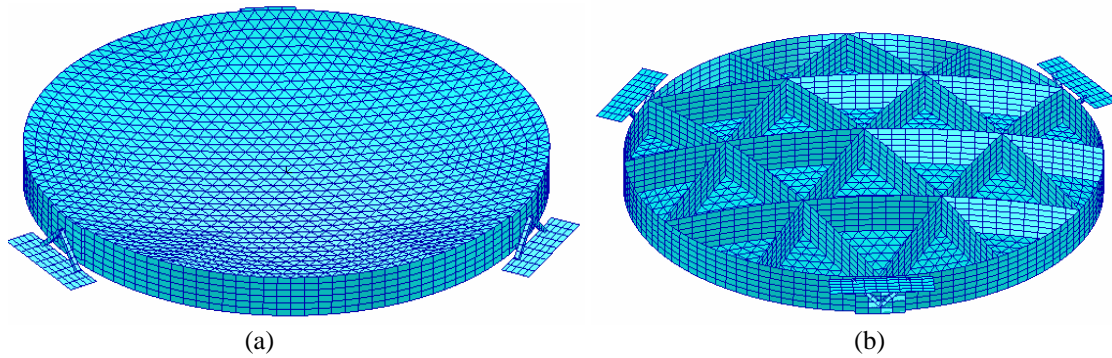


Figure 1: Lightweight mirror with 3 edge mounts  
 (a) top view, (b) bottom view

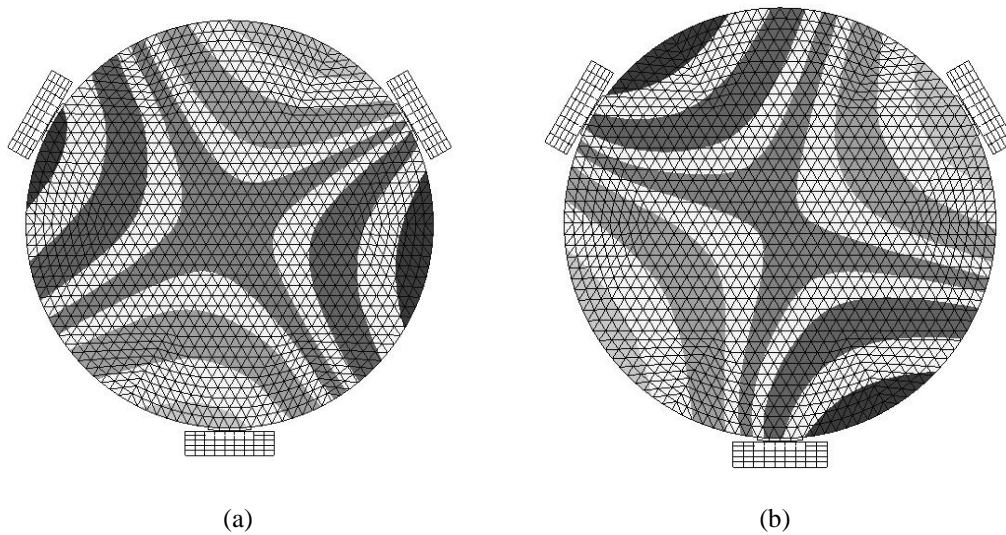


Figure 2: Surface deformations with Best-Fit plane removed  
 (a) radial rotation of mount, (b) z offset of mount

For the Monte Carlo analysis in SigFit, the random variables were assumed to be uniformly distributed over the range of plus to minus the input value (i.e. for flatness the slopes range from +0.0001 to -0.0001 radian). SigFit results include mean, standard deviation, maximum value, minimum value and user specified percentile. In Table 1 below, the 90 percentile results are presented for surface RMS and the amplitude of the low order Zernikes for 1000 sets of random variables. The units used in the table are waves HeNe (0.6328 microns). The table shows that 0.0020 inch of coplanarity is much more significant than the slope errors. Also, the dominate response is primary astigmatism with very little power amplitude. This approach can be used to determine realistic mechanical tolerance based on optical response quantities.

90 percentile results from 1000 Monte Carlo analyses			All terms	Radial Flatness	Circumf Flatness	Co- planarity
			9 variables (waves)	3 variables (waves)	3 variables (waves)	3 variables (waves)
N	M	RMS (-BFP)	0.02762	0.00648	0.00104	0.02737
2	0	Power (Defocus)	0.00020	0.00000	0.00021	0.00000
2	2	Pri Astigmatism-A	0.04532	0.01500	0.00145	0.04280
2	2	Pri Astigmatism-B	0.04410	0.01543	0.00160	0.04413
3	1	Pri Coma-A	0.00038	0.00001	0.00007	0.00037
3	1	Pri Coma-B	0.00038	0.00001	0.00006	0.00039
3	3	Pri Trefoil-A	0.00175	0.00390	0.00000	0.00000
3	3	Pri Trefoil-B	0.00022	0.00000	0.00023	0.00000
4	0	Pri Spherical	0.00004	0.00000	0.00004	0.00000
4	2	Sec Astigmatism-A	0.00235	0.00080	0.00011	0.00237
4	2	Sec Astigmatism-B	0.00229	0.00087	0.00011	0.00226
4	4	Pri Tetrafoil-A	0.00255	0.00055	0.00009	0.00253
4	4	Pri Tetrafoil-B	0.00247	0.00057	0.00008	0.00246

Table 1: Mount flatness results from Monte Carlo analyses

#### 4.0 COEFFICIENT OF THERMAL EXPANSION VARIABILITY REQUIREMENT

Variability of CTE can be a significant cause of mirror surface distortion. The variability can come from boule to boule of glass, or within a single boule there may be variation through the thickness or radially. When a lightweight mirror is fabricated, the variation can be distributed through the front and rear faceplates and core structure. For segmented mirrors, these variations will occur from segment to segment. In the following simple example (Figure 3), the CTE in each segment is treated as a normally distributed variable. The FE model was run with a unit thermal load on each segment as a separate subcase. These subcases were brought into SigFit for a Monte Carlo analysis.

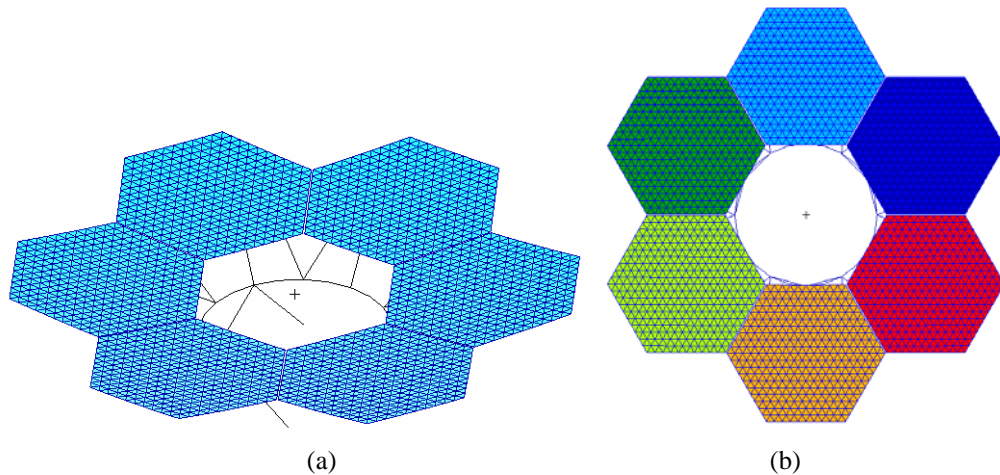


Figure 3: (a) segmented mirror model, (b) CTE variation by segment

If the mean CTE was zero with a standard deviation of 1 ppm, then the Monte Carlo results for 10,000 analyses are shown in Table 2. Since the driving force in each subcase is the product of CTE and temperature, this analysis

procedure could be used to determine thermal control requirements rather than CTE requirements, or in combination with CTE requirements.

Surface	Mean	StDev	Max	95%	5%	Min
RMS	1.37	0.48	3.53	2.23	0.66	0.15

Table 2: Monte Carlo analysis results on surface RMS error due to CTE variation

## 5.0 ADAPTIVE MIRROR ACTUATOR RESOLUTION REQUIREMENT

Adaptive mirror analysis is usually conducted with continuously variable actuator strokes. In reality, actuators have a resolution which limits their accuracy. To understand the effect of actuator resolution, a Monte Carlo analysis can predict residual surface RMS caused by resolution limits. The adaptive mirror shown in Figure 4 is sitting on a 3 point mount with 15 force actuators. For a 1g axial gravity load ( $RMS = 3.00\lambda$ ), the actuators are able to correct 98% of the elastic distortion resulting in  $RMS = 0.052\lambda$ . If the force actuators had a resolution of  $\pm 0.10$  Lb, the Monte Carlo analysis predicts the mean residual surface error would increase to  $0.060\lambda$  and the 95 percentile surface error would be  $0.079\lambda$ . The analysis results can be used to determine the actuator resolution required to meet optical performance requirements on surface RMS.

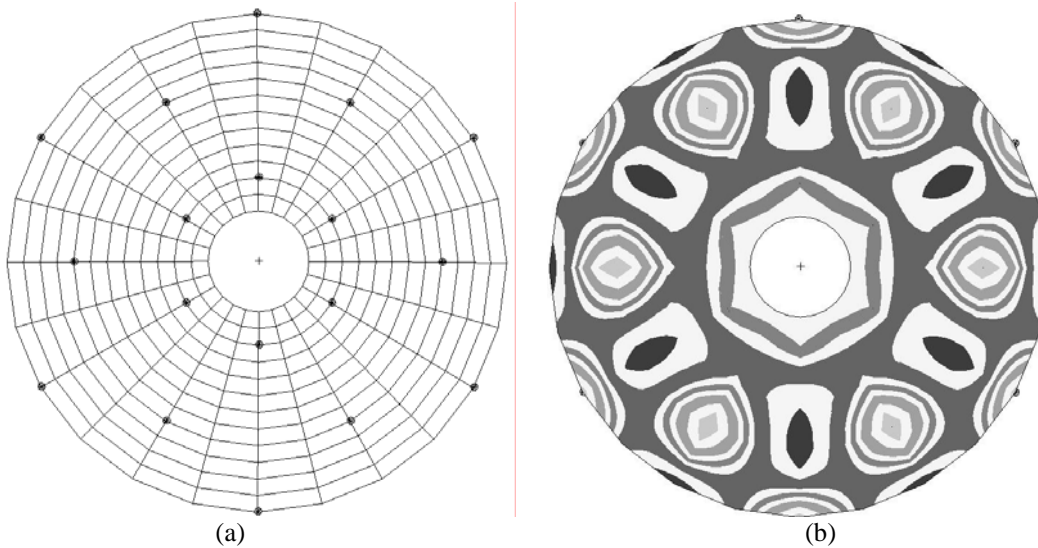


Figure 4: Adaptive mirror model  
(a) model with actuators, (b) 1g deformation corrected by actuators

## 6.0 TELESCOPE LINE-OF-SIGHT REQUIREMENT

A simple telescope in Figure 5 has long composite tubes supporting the secondary mirror assembly. It may be necessary to determine the requirement on coefficient of thermal expansion (CTE) variability of the tubes. A finite element model was run with 9 loadcases, each representing a CTE variation of a single tube. The variations considered were uniform CTE variation, linear gradient in radial direction (long dimension of the cross-section) and a linear gradient in the circumferential direction (short dimension of the cross-section). Deformed plots for a single loadcase are shown in Figure 6. For specific (known) CTE variations the results can be linearly combined to give the net effect. For unknown CTE variations treated as random variables, the results must be combined using Monte Carlo techniques. Both the line-of-sight (LoS) calculation and the Monte Carlo simulation were run in SigFit.

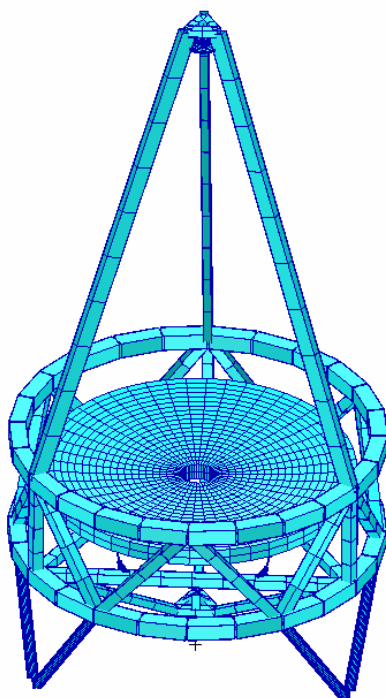


Figure 5: Simple telescope model

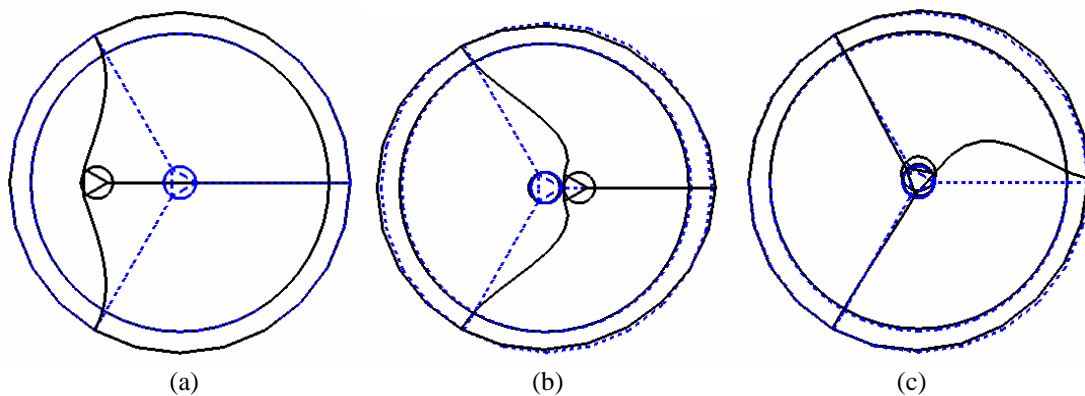


Figure 6, Deformed shapes for CTE variations on a single strut  
(a) uniform, (b) radial gradient, (c) circumferential gradient

The results of the Monte Carlo simulation of 1000 variations are given in Table 3. As expected, the uniform CTE has the largest effect. This tool could now be used to specify allowable tolerances on the CTE variability to maintain LoS error within required limits.

LoS Error (mm) per degree C				
CTE Variations	Mean	StDev	Max	90%-tile
All 3 Var	0.0251	0.0116	0.0615	0.0406
Uniform Var only	0.0238	0.0108	0.0515	0.0385
Radial Var only	0.0069	0.0031	0.0148	0.0111
Circumf Var only	0.0022	0.0010	0.0048	0.0036

Table 3: LoS error for 1000 random variations

## 7.0 SIGFIT CAPABILITIES OVERVIEW

SigFit is a general purpose optomechanical analysis program. The most common use of SigFit is to fit polynomials to deformed surfaces<sup>3,4</sup>. SigFit offers a wide variety of surface geometries as shown in Table 3. The conic geometry may add any of the polynomial types listed. For each surface shape the optical segment may represent an arbitrary off-axis portion of the parent geometry, allowing a wide variety of ‘free form’ optics to be analyzed. Disturbances to be analyzed (fit) include the types listed plus arbitrary linear combinations. SigFit writes the polynomials to files for direct input to the optics programs listed. In addition to fitting polynomials, SigFit can interpolate disturbances to rectangular grid arrays for input to optics programs or interferometers.

Surface Shapes	Polynomials	Disturbances	FE Programs	Optics Programs
Flat	Zernike	Finite element results	Nastran (all)	CodeV
Conic	Fringe Zernike	Polynomials	Ansys (all)	Zemax
Biconic	Annular Zernike	Vector data	Abaqus	Oslo
Anamorphic	Asphere	Interferogram arrays	Cosmos	Interferometers
Grazing conic	Forbes QCON	Combinations of above		
Ogive	Forbes QBFS			
Conic+any poly	XY			
Offset segments	Legendre			
	Fourier-Legendre			

Table 3: Summary of SigFit fitting capabilities

For adaptive optics, SigFit solves for actuator strokes to minimize surface RMS. In addition, SigFit will use genetic optimization<sup>5</sup> to find the best actuator locations to correct multiple load cases. There are unique capabilities within SigFit for dynamic analysis (harmonic, random, transient) of optical systems. For instance, the MTF effect of jitter can be determined in random response analysis. Key mode contributors to line-of-sight jitter are identified as well as individual surface contributors. SigFit can also analyze thermo-optic effects (change in index with temperature) and stress-optic effects (change of index due to stress and stress birefringence).

## 8.0 SUMMARY

Monte Carlo techniques have been combined with integrated optomechanical analysis tools to determine mechanical tolerances based on optical performance measures, such as surface RMS and line-of-sight errors. The examples included in this paper of mount flatness, material property variability, thermal control tolerance and actuator resolution, show the wide applicability and usefulness of the tool.

## REFERENCES

- [1] SigFit Reference Manual, Sigmadyne, Inc., Rochester, NY, 2011. (2011)
- [2] Doyle, K., Genberg, V., Michels, G., Integrated Optomechanical Analysis, SPIE, TT58, (2002)
- [3] Genberg, V., Doyle, K. and Michels, G., “An optical interface for MSC Nastran,” MSC Conference Proc VPD04-31, (2004).
- [4] Michels, G., Genberg, V., and Doyle, K., “Integrating ANSYS mechanical analysis with optical performance analysis with SigFit,” ANSYS User Conference Proc., (2008).
- [5] Michels, G., Genberg, V., Doyle, K., and Bisson, G., “Design optimization of actuator layouts of adaptive optics using a genetic algorithm,” Proc. SPIE 5877-22, (2005).